Published in final edited form as:
Matrix Biol. 2009 April ; 28(3): 148–159. doi:10.1016/j.matbio.2009.02.002.

Matrix metalloproteinase-9 deficiency leads to prolonged foreign body response in the brain associated with increased IL-1β levels and leakage of the blood brain barrier

Weiming Tian and **Themis R. Kyriakides**
Vascular Biology and Therapeutics Program. Departments of Pathology and Biomedical Engineering, Yale University, New Haven CT 06519

Abstract

Matrix metalloproteinases (MMPs) are enzymes with specificity towards extracellular matrix (ECM) components. MMPs, especially MMP-9, have been shown to degrade components of the basal lamina and disrupt the blood-brain barrier (BBB) and thus, contribute to neuroinflammation. In the present study we examined the role of MMP-9 in the foreign body response in the brain. Millipore filters of mixed cellulose ester were implanted into the brain cortex of wild type and MMP-9 -null mice for a period of 2 d to 8 wks and the response was analyzed by histology and immunohistochemistry. We observed enhanced and prolonged neuroinflammation in MMP-9-null mice, evidenced by persistence of neutrophils, macrophages/microglia, and reactive astrocytes up to 8 wks post-implantation. In addition, blood vessel density around implants was increased in MMP-9-null mice and detection of mouse serum albumin (MSA) indicated that vessels were leaky. Immunohistochemical and western blot analyses indicated that this defect was associated with the absence of tight junction proteins zonula occludens-1 (ZO-1) and ZO-2 from vessels in proximity to implants. Analysis of brain sections and brain protein extracts revealed that the levels of the pro-inflammatory cytokine interleukin-1β (IL-1β), which is a substrate for MMP-9, were significantly higher in MMP-9-null mice at 8wks post-implantation. Collectively, our studies suggest that increased levels of IL-1β and the delayed repair of BBB are associated with prolongation of the FBR in MMP-9-null mice.

Keywords

Matrix metalloproteinase; foreign body response; biomaterials; neuroinflammation; blood-brain barrier; interleukin

Introduction

Matrix metalloproteinases (MMPs) are a family of highly homologous protein-degrading zinc-dependent endopeptidases that can be divided into collagenases (MMP-1, -8, and -13), gelatinases (MMP-2 and 9), stromelysins (MMP-3 and 10), matrilysins (MMP-7 and 26), and the membrane-type MMPs (MMP-14-17 and 24) (Visse and Nagase, 2003). MMPs are

Corresponding author: Themis R. Kyriakides, Ph.D., Yale University School of Medicine, Amistad Research Building, 10 Amistad Street, Room 301C, P.O. Box 208089, New Haven, CT 06520, Phone: (203) 737-2214, Fax: (203) 737-2293, themis.kyriakides@yale.edu.

important in many biological processes including embryonic development (Canete-Soler et al., 1995; Kinoh et al., 1996), angiogenesis (Vu et al., 1998), wound healing (Kyriakides and Bornstein, 2003), inflammation (Parks et al., 2004), and cancer (Overall and Lopez-Otin, 2002). In addition, MMPs are mediators of pathology and regeneration of the central nervous system (CNS) and their activities have been shown to have both beneficial and detrimental effects (Agrawal et al., 2008; Nagase and Woessner, 1999; Yong, 2005). For example, MMP-9 has been shown to degrade components of the basal lamina, leading to disruption of the blood-brain barrier (BBB), and to contribute to the neuroinflammatory response in many neurological diseases (Kieseier et al., 1999; Lindberg et al., 2001). Furthermore, MMP-9 activity has been shown to increase in traumatic brain injury (TBI) and spinal injury models (Wang et al., 2000; Noble et al., 2002). By degrading neurovascular matrix, MMP-9 promotes injury of the blood–brain barrier leading to hemorrhage and edema formation (Mun-Bryce and Rosenberg, 1998; Shigemori et al., 2006). In addition, MMP-9 triggers neuronal and glial cell death by disrupting cell–matrix signaling and homeostasis (Gu et al., 2002; Lee and Lo, 2004). Studies in MMP-9-null mice have supported the notion that MMP-9 plays an important role in neuronal repair. Specifically, in a model of spinal injury contusion, MMP-9-null mice suffered fewer motor deficits and smaller contusion volumes compared with WT mice (Noble et al., 2002). In spinal cord injury, MMP-9-null mice exhibited decreased disruption of the blood–spinal cord barrier leading to attenuation of neurotrophil infiltration and better locomotor recovery (Lo et al., 2003). In addition, double MMP-2/MMP-9 null mice displayed resistance to experimental autoimmune encephalomyelitis (EAE) due to reduced leukocyte infiltration (Agrawal et al., 2006). Collectively, these studies suggest that MMP-9 might play a negative role in the repair of the CNS, hence, investigators have pursued the development of MMP inhibitors for the treatment of acute neural injuries (Sood et al., 2007; Yang et al., 2007). However, MMPs have also been shown to have beneficial effects in the CNS such as supporting neurogenesis, growth and regeneration of axons, myelogenesis, angiogenesis, and resolution of neuroinflammation (Cunningham et al., 2005)Yong, 2005). For example, a study showed that inhibition of MMPs, particularly MMP-9, hinders brain repair in a stroke model in mice and may increase the risk for intra-cerebral bleeding (Zhao et al., 2006). Moreover, in a model of collagenase-induced intracerebral hemorrhage and brain injury MMP-9-null mice suffered increased hemorrhage and brain edema and neurological deficits (Tang J 2004).

In the present study, we investigated the role of MMP-9 in the foreign body response (FBR) in the brain. With the advent of brain implantable devices, such as stimulating electrodes and recording electrode arrays, the identification of specific molecular determinants of the ensuing foreign body response is critical for the development of biologically-based surface modification strategies. In general, biomaterials, medical devices, and tissue engineered constructs induce a FBR that is characterized by the formation of a collagenous capsule that aims to isolate the implant from the surrounding tissue (Anderson et al., 2008). In the brain, the FBR is characterized by the presence of both reactive astrocytes, which form a glial scar, and activated microglia (Fournier et al., 2003; Kim et al., 2004), and has shown to be the main cause of failure of brain electrode arrays (Biran et al., 2005; Polikov et al., 2005). Variations in electrode design and implantation method have been shown to influence the extent of the early (1 wk) inflammatory response in the rat (Szarowski et al., 2003). However, after 4 wk all experimental groups displayed similar FBR. In a separate study, silicon-based electrode coated with laminin induced an increased and decreased FBR in the rat brain in comparison to uncoated electrodes during the early (1 d) and late (4 wk) response, respectively (He et al, 2006).

A study has suggested that MMPs might be important in the fusion of macrophages to form foreign body giant cells in vitro (Jones et al, 2008). We recently showed in *in vivo* studies

involving subcutaneous implants that MMP-9 is critical for macrophage fusion and proper assembly of extracellular matrix during the FBR (Maclauchlan et al, 2009). Here, we investigated the expression of MMP-9 during the FBR in the brain using a Millipore filter (mixed cellulose ester) implant model and compared the response between wild type (WT) and MMP-9-null mice. Previously, we have shown that this material induces a normal foreign body response and behaves exceptionally well during histological processing (Kyriakides et al., 2004; Maclauchlan et al, 2009). We found that the latter displayed prolonged neuroinflammation up to 8 wks post implantation, which was associated with prolonged leakage of the BBB barrier, increased levels of IL-1β, and loss of tight junctions proteins in vessels. Collectively, our findings show that MMP-9 is required for the repair of the BBB and expedient resolution of the FBR in the brain.

Results

MMP-9 in the brain following implantation

Immunohistochemical detection of MMP-9 in brain sections revealed its deposition in the proximity of implants. Specifically, immunoreactivity was prominent from 2 d to 2 wk (Figure 1 A-C). MMP-9 deposition declined by 4 wks (Figure 1 D) and was almost undetectable at 8wk (Figure 1 E). No immunoreactivity was detected in sections of brain without implant (not shown) and in MMP-9-null brain 2 d following implantation (Figure 1 F, negative control). Double immunofluorescence analysis of 2 wk implants revealed extensive and limited co-localization of MMP-9 with F4/80-positive cells and GFAP-positive cells, respectively, suggesting that inflammatory macrophages are a major source of MMP-9 (Figure 2). In addition, western blot analysis of MMP-9 in brain extracts revealed levels similar to those observed by immunohistochemical analysis (Figure 2 G). Zymographic analysis of 4 wk brain protein extracts revealed normal levels of MMP-2 in MMP-9-null mice, suggesting the lack of compensatory upregulation of MMP-2 (Supplemental Figure 2).

Enhanced neuroinflammation in the FBR of MMP-9-null mice

Examination of H&E-stained sections revealed the pronounced inflammatory cell infiltration following implantation in both WT and MMP-9-null mice (Figure 3). At 2 d, hemorrhage was observed in both animals, indicating that the implantation caused damage to blood vessels. Examination of implants at 4 and 8 wk indicated resolution of inflammation in WT mice (Figure 3 C, E). In contrast, MMP-9-null mice displayed prolonged neuroinflammation that persisted until at least 8 wk, the latest time point we examined.

Because the inflammatory response to materials implanted in the CNS has been shown to involve multiple cell types, we proceeded to analyze sections by immunohistochemistry for the presence of macrophage/microglia and neutrophils with F4/80 and 7/4 antibodies, respectively. In MMP-9-null brain the presence of both neutrophils and macrophage/microglia was greatly increased in comparison to WT at 8 wk (Figure 4 B, D). Quantification of the number of neutrophils and macrophage/microglia from digital images revealed a trend for increased inflammation between 2-14 days following implantation in WT brain (Figure 4 E, F), which was followed by progressive decrease between 4 and 8 wks. In MMP-9-null brain, neutrophils remained relatively unchanged between 2 d and 4 wk whereas the presence of microglia/macrophage kept increasing during the same period. The latter is a major glial cell type involved in the inflammatory response, constituting 5–10% of the total number of glial cells in the brain (Polikov et al., 2005). Therefore, the increased presence of F4/80-positive cells around the implant suggests the induction of a robust and persistent inflammatory response.

Enhanced astrocyte reaction and angiogenesis in the FBR of MMP-9-null mice

GFAP immunostain was performed to detect astrocytes and to determine the extent of "reactive gliosis", the term used to describe the activation, hypertrophy, and proliferation of astrocytes in response to injury. Numerous reactive astrocytes were found around the implant. Consistent with our findings on the inflammatory response, we detected an increase in GFAP reaction following implantation, which increased for the first 2 wk in both groups. However, unlike WT mice that progressed towards resolution (Figure 5 E), MMP-9-nul mice displayed extensive reactive gliosis at 8 wks (Figure 5 B). The persistent of reactive astrocytes at 8 wk was not observed in MMP-9-null mice that were subjected to sham injury (Supplemental Figure 3). Collectively, our observations suggest that MMP-9-null mice are unable to resolve the inflammatory and subsequent repair responses that are elicited by biomaterial implantation. In addition, we determined the extent of angiogenesis by immunodetection of von Willebrand Factor (vWF) (Figure 5 C, D). Quantification of blood vessels indicated similar angiogenic responses in WT and MMP-9-null mice at 2 and 4 wk (Figure 5 F). However, unlike WT mice, MMP-9-null displayed a pronounced increase in blood vessel density at 8 wk. In addition to the number of blood vessels, we determined the average diameter and area of each blood vessel and found no significant differences between WT and MMP-9-null mice (data not shown).

Increased IL-1β levels in MMP-9-null mouse brain

To investigate the enhanced neuroinflammation we employed western blot analysis of brain extracts to compare the levels IL-10 between WT and MMP-9-null mice and found them to be similar (not shown). In contrast, immunoprecipitation analysis revealed that the levels of the pro-inflammatory cytokine IL-1β were elevated in MMP-9-null brain (Figure 6 E). In addition, immunohistochemical analysis coupled with histomorphometry revealed increased IL-1β deposition at 8 wk in the vicinity of implants in MMP-9-null brain (Figure 6 B, C). Moreover, ELISA analysis revealed an approximate five-fold increase in the levels of IL-1β in 8 wk MMP-9-null samples in comparison to WT (Figure 6 D).

Prolonged BBB leakage in MMP-9-null mice

We analyzed the integrity of the BBB in WT and MMP-9-null mice by detecting MSA whose absence from the brain parenchyma is a reliable measure for BBB integrity (van Vliet et al., 2007). Lack of MSA immunoreactivity indicated no leakage in the cerebral cortex controlateral from the implant site or in mice that did not receive implants, indicative of a structurally intact BBB (Figure 7 A, B). In contrast, high level of MSA immunoreactivity was detected 2 d following implantation in WT and MMP-9-null mice (Figure 7 C, D). Examination of the MSA levels over time indicated progressive decrease from 2 d to 8 wk in WT mice (Figure 6 E). In contrast, MMP-9-null mice displayed an initial decrease followed by an increase between 2-8 wk (Figure 7 F). The increased MSA levels at 8wk in MMP-9-null mice were verified by histomorphometric evaluation (Figure 7 G). Similar to our findings with GFAP detection, MMP-9-nul mice subjected to sham injury did not exhibit excessive BBB leakage at 8 wk (Supplemental Figure 3).

The BBB involves a number of mechanisms that control the composition of the neurochemical environment around neurons and glia, which are essential for the normal function of the CNS (Kim et al, 2004). Part of this mechanism involves the formation of intercellular tight junctions between endothelial cells that prevent molecules from passing into the CNS (Ek et al., 2006). We examined the presence of the tight junction proteins ZO-1 and ZO-2 by immunohistochemistry and found that, unlike WT vessels, both ZO-1 and ZO-2 were absent form the blood vessels adjacent to the implants at 8 wk in MMP-9-null mice (Figure 8 D, H). At this time point, the lack of ZO-1 and ZO-2 was only observed in vessels within 200 μm of implants. In contrast, both proteins were detected in vessels that

were at least 200 μm away from the implants in MMP-9-null mice and in all vessels of WT mice (Figure 8). Western blot analysis of 8 wk brain extracts revealed the reduced levels of ZO-1 and ZO-2 in MMP-9-null samples (Figure 8 I, J).

Discussion

In the present study we investigate the role of MMP-9 the brain FBR and discovered that MMP-9-null mice display increased and prolonged neuroinflammation and glia reaction as well as prolonged disruption of the BBB. Induction of the FBR in WT mice resulted in increased deposition of MMP-9, which was detected from 2 d to 8 wk. The early detection of MMP-9 is consistent with findings in a traumatic brain injury model where MMP-9 levels were shown to increase as early as 3 h after trauma, peaked at 24 hr, and remained elevated for the duration of the experiment, which was 1 wk (Wang et al., 2000). Here we show that in the FBR the deposition of MMP-9 can be sustained for 4-8 wk, suggesting that the presence of the implant leads to conditions that cause the persistence of MMP-9 in the brain tissue. We believe this to be a relevant issue since the inflammatory and astrocyte responses to trauma in MMP-9-null brain, unlike in the FBR, can resolve at 8 wk (Supplemental Figure 3). Taken together, these observations suggest that there is a unique requirement for MMP-9 in the brain FBR.

Several studies have investigated aspects of the brain FBR, mostly in rat models, following the implantation of electrodes (Reviewed in (Polikov et al., 2005)). Notably, Szarowski et al have shown strong reactive glia response following the implantation of silicon-based electrodes in the rat brain (Szarowski et al., 2003). In contrast to our findings, these investigators reported prolonged FBR in immunocompetent rats lasting at least 12 wk based on the presence of reactive astrocytes and macropahes/microglia. Possible explanations for the distinct findings include differences in the brain FBR between rats and mice and, most likely, differences between the mechanical properties of the implants (silicon versus mixed cellulose ester). Mismatches in mechanical compliance between biomaterials and brain tissue have been suggested to play a role in the FBR (Cheung, 2007). Thus, disparities in the Young's modulus (170 Gpa for silicon electrodes and approximately 2 Gpa for cellulose filters) could have a significant impact in the FBR. In a separate study, He et al showed that silicon electrodes coated with laminin elicited a somewhat dampened FBR at 4 wk following implantation, characterized by reduced astrocytic and macrophage/microglia responses (He et al., 2006). This study highlights the potential benefit of biological modulation of the brain FBR. However, despite the decreased FBR, no changes in the density of neurons near the two types of implants could be observed prompting the investigators to conclude that modulation of additional factors is needed.

Local integrity of the BBB can be disrupted following mechanical (Noble and Wrathall, 1989), chemical (Yoshizumi et al., 1993), thermal (Mitchell et al., 1979; Nag et al., 2001; Wijsman and Shivers, 1993), metabolic (Gross et al., 1986; Jacobs et al., 1992), and osmotic (Kajiwara et al., 1990) insults to the central nervous system. The time course of BBB repair correlates with the severity of the primary injury and with secondary pathological changes. The latter are related to vascular hemorrhage and edema formation (Stolp et al., 2005; Tator and Fehlings, 1991) that evoke a cascade of inflammatory responses including macrophage invasion (Beck et al., 1983; Blight, 1994). In mechanical injury models in rodents, the disrupted BBB is repaired within 10 to 14 d (Faulkner et al., 2004). However, BBB repair required 7-8 wk in a polymer capsule implantation model in the rat (Jaeger et al., 1991). Our finding of complete repair of the BBB between 4-8 wk following implantation is consistent with this study. Taken together, these observations suggest that implantation models cause a longer disruption of the BBB. We postulate that, unlike injury models where inflammation

can resolve, the FBR presents a continuous stimulus for inflammation that interferes with the restoration of the BBB.

Intracorporeal implanted biomaterials and medical devices induce a FBR that consists of a series of overlapping phases including inflammation, foreign body giant cell formation, and formation of a collagenous capsule that surrounds the implant (Polikov et al, 2005). In animal models, the FBR displays an active inflammatory/phase that peaks at 2 wk and appears to stabilize by 4 wk. We observed a similar time course in the FBR in the brain, even though the resulting reaction differs from that seen in other tissues. For example, we did not detect giant cell formation in any of our implants. Furthermore, reactive gliosis instead of a dense collagenous capsule surrounds brain implants (Fournier et al., 2003). Differences at the cellular level also distinguish the FBR in the brain where implantation causes the recruitment and activation of cells such as neutrophils, macrophages, microglia, and astrocytes. Increased and prolonged presence of all these cell types in MMP-9-null mice suggests aberrant regulation of neuroinflammation, a process that has been shown to involve MMPs (Yong, 2005). For example, it was shown that MMPs contribute the enhancement of neuroinflammation by generating encephalogenic fragments from CNS proteins such as myelin basic protein (Proost et al, 1993). In addition, studies have implicated MMPs in the resolution of inflammation. Specifically, in an allergen-induced airway inflammation model, MMP-9 deficiency resulted in enhanced inflammation (McMillan et al., 2004). Moreover, MMP-9-null mice were shown to be unable to resolve contact dermatitis due, in part, to a failure to generate the regulatory cytokine IL-10 (Wang et al, 1999). We pursued the possibility that IL-10 deregulation might be involved in the prolonged neuroinflammation in MMP-9 -null mice but we found normal IL-10 levels in MMP-9-null brain by western blot (data not shown). MMP-9 can also act on the pro-inflammatory cytokine IL-1β in a biphasic fashion by leading to its activation and subsequent degradation, and thus facilitate the resolution of neuroinflammation (Ito et al, 1996; Schonbeck et al., 1998). We analyzed the deposition and levels of IL-1β and found that they were increased in MMP-9-null mice at 8 wk post-implantation. Thus, the increase in IL-1β is associated with prolongation of the FBR. Specifically, IL-1β can delay neutrophil apoptosis (Coulter et al., 2002; Coxon et al., 1999), thus impairing the resolution of the inflammatory response. Consistent with this suggestion, a recent study involving a ventilator-induced lung injury model demonstrated an increase in neutrophil influx in MMP-9-null mice (Albaiceta et al., 2008). Furthermore, the increase in IL-1β could also explain the prolonged BBB leakage MMP-9-null mice because it has been shown to regulate the permeability of the BBB and to induce loss of the tight junctional proteins, occludin and ZO-1 (Bolton et al, 1998). In addition, IL-1β could increase permeability via reactivation of the hypoxia-angiogenesis program (Argaw et al., 2006).

Based on the prolonged presence of GFAP immunoreactivity we conclude that the astrocyte reaction and reactive gliosis are enhanced in MMP-9-null mice. A recent study demonstrated that MMP-9 deficiency did not influence glial scar formation in a transient focal cerebral ischemia model (Copin and Gasche, 2007). Specifically, reactive astrocytes were detected from d 1 to 3 wk and the levels were similar between WT and MMP-9-null mice. We believe the reason for the different observation in our implantation study is the prolonged microglia/macrophage due to the presence of the implant. This suggestion is consistent with a previous study that demonstrated a correlation between the occurrence of astrogliosis and the presence of reactive microglia/macrophages (Balasingam et al, 1996).The increased presence of astrocytes and inflammatory cells might also explain the increased angiogenesis in MMP-9-null mice. Previous studies have confirmed that astrocytes can promote angiogenesis (Laterra et al., 1990; Suarez et al., 1994). Furthermore, studies have shown that astrocytes release arachidonic acid and cytochrome P-450 epoxygenase products, known as

epoxyeicosatrienoic acids, which have been shown to have many mitogenic and cell-growth-related activities (Medhora and Harder, 1998; Murphy et al., 1988).

A number of studies have shown that MMP-9 could increase the permeability of BBB by degrading tight junction components such as ZO-1 (Asahi et al., 2001). Furthermore, inhibitors of MMPs have been shown to reduce the permeability of the BBB during many pathological conditions (Sood et al., 2008; Yang et al., 2007). However, a study showed that MMP-9 deficiency does not decrease but rather increases vasopermeability (Kolaczkowska et al., 2006). Furthermore, in a stroke model in the rat, it was shown that immediate inhibition of MMPs conferred neuroprotection, whereas delayed inhibition at 7 d increased stroke volume (Zhao et al., 2006). The authors emphasized the need to evaluate long-term effects of MMP inhibitors in acute brain injury models.

Finally, there might be a correlation between prolonged neuroinflammation and BBB leakage in MMP-9-null mice. The BBB functions to restrict the passage of macromolecules, and perhaps cells, into the CNS. In pathological conditions, the BBB may become leaky and the leakage of macromolecules might facilitate the passage of leukocytes into the CNS, a process believed to be an early event in the pathogenesis of MS and AIDS encephalitis (Williams and Hickey, 1995). BBB impairment during CNS inflammation is believed to result from disruption of junction complexes between brain microvascular endothelial cells with subsequent formation of a paracellular route that facilitates entry of leukocytes into the brain parenchyma. Although other pathways for leukocyte migration have been proposed (e.g., transcytosis), both experimental and clinical observations point to the importance of the paracellular route in leukocyte entry and across BBB during CNS inflammation (Schenkel et al., 2004). More importantly, in a model of EAE it was shown that double MMP-2/MMP-9-null leukocytes were unable to cleave the transmembrane receptor dystroglycan, which is a required event to disrupt the interaction of astrocyte endfeet with the parenchymal basement membrane (Agrawal et al, 2006). Loss of MMP-2 and MMP-9 conferred resistance to EAE due to reduced leukocyte-induced disruption of the BBB. Our study differs from the EAE model in that the disruption of the BBB is primarily due to mechanical damage during implantation. Moreover, our study suggests that MMP-9 is critical for proper restoration of the BBB. Thus, in our experiments MMP-9-null leukocytes, which still can express MMP-2, can infiltrate due to a compromised BBB. Interestingly, aged MMP-9-null mice were shown to suffer increased hemorrhage and brain edema in a model of collagenase-induced intracerebral brain injury, which was associated with enhanced expression of MMP-2 and MMP-3 (Tang et al, 2004). Thus, in an MMP-9 deficient state conditions can exist that can lead to increased leakage of the BBB.

In the present study we show that MMP-9 can be detected during the FBR in the brain and that the process is prolonged in MMP-9-null mice. Specifically, the prolongation is associated with excessive neuroinflammation, increased reactive gliosis, disrepair of the BBB, and elevated levels of the pro-inflammatory cytokine IL-1β. In contrast, MMP-9-null mice are capable of resolving inflammation following brain injury, indicating the existence of a unique requirement for MMP-9 in the FBR. Furthermore, our studies demonstrate substantial and prolonged leakage of the BBB in the FBR, even in WT animals, suggesting that this parameter should be measured in studies evaluating the biocompatibility of materials for application in the CNS.

Materials and methods

All animal studies were approved by the Institutional Animal Care and Committee of Yale University. 40 MMP-9-null mice and 40 WT mice, both in the FvB/NJ genetic background, were used in this study. MMP-9-null mice share approximately 95% identity with FvB/NJ

(Wang et al., 2008). To generate WT mice in a background almost identical to that of MMP-9-null mice, WT (FvB/NJ) mice were bred to MMP-9-null mice and the resulting heterozygotes were bred to generate WT mice. 3-mo old mice were anesthetized via IP administration of 100 mg/kg ketamine and 10mg/kg xylazine and immobilized in a mouse head holder (921-E Davidkopf Instruments). The calvarium was exposed by a midline scalp incision from the nasion to the superior nuchal line, and then the skin was retracted laterally. With a variable speed drill (Ideal Micro-drill), a 2.0-mm burr hole was made 1.0 mm posterior to the bregma and 3.0 mm to the right of midline over the left hemisphere. Sterile 2 × 2 mm pieces of Millipore filter (mixed cellulose ester, 150 μm thick and 0.45 μm pore size), one per animal, was inserted into the brain cortex via a stereotactic device and removed at specific time points ranging from 2 d to 8 wks post implantation (Supplemental Figure 1 shows exact location of implants). For all WT and MMP-9-null mice, tissues were harvested on d 2 and 1, 2, 4, and 8 wk (5 mice for each time point per genotype). A sham group where an implant was inserted and removed immediately was also analyzed.

Histology and Immunohistochemistry

For perfusion-fixation of implants, mice were administered 100 mg/kg ketamine and 10 mg/kg xylazine IP to induce relaxation. Subsequently, mice were transcardially perfused with 0.1 M PBS (30 ml) and then with 4 % paraformaldehyde in phosphate buffer (25 ml) at 4°C. Brains were removed, post-fixed overnight in the same fixative at 4 °C, and then cryoprotected for 24–48 h in a solution of sucrose 30% in PBS at 4°C. Processed tissues were then embedded in paraffin and serially sectioned (6 μm thick) in the horizontal plane across the implantation site. Selected tissues were prepared without fixation and stored at -80°C and used to generate protein extracts. The position of the implant and the areas isolated for tissue processing and protein extraction are shown in Supplemental Figure 1.

Paraffin sections were stained with hematoxylin-eosin (H&E) according to standard protocol. For immunohistochemical analysis, sections were incubated in 3% H_2O_2 to quench endogenous peroxidase. Detection of MMP-9 (R&D system; 1:100) and F4/80 (Serotec, 1:100) required antigen retrieval by heating slides for 30 min at 100°C in citrate buffer (pH 6). For detection of vWF (Abcam; 1:400) and Zonula occludens (ZO-1) (Zymed Laboratories; 1:100) antigen retrieval was performed by digestion with proteinase K (10 min at 37°C). For detection of IL-1β, the sections were heated in 6M urea for 30 min at 95-100°C. Detection of GFAP (Zymed Laboratories; 1:50), 7/4 neutrophil (Abcam; 1:400), ZO-2 (Zymed Laboratories; 1:100), and MSA (Abcam; 1:5000) was performed without antigen retrieval. All primary antibodies were diluted with 1% BSA in PBS. Biotinylated secondary antibodies were used at a dilution of 1:200. For light microscopy antibody reactions were visualized with the ABC kit (Vector Laboratories) and all slides were counterstained with methyl green. For the anti-MMP-9 Ab, sections from MMP-9-null brain served as negative control. For all other antibodies, selected sections were stained only with secondary antibodies to evaluate the extent of non-specific antibody interactions. For double immunohistochemistry, MMP-9 immunoreactivity was detected with a FITC-conjugated secondary IgG and GFAP and F4/80 with a TRITC-conjugated secondary IgG.

Histomorphometry

All images were captured with the aid of a Nikon Eclipse 80i microscope with NIS-Elements D 2.30 software. The number of inflammatory cells and blood vessels were determined by manual counts from high power digital images. GFAP distribution and mouse serum albumin (MSA) extravasation into brain tissue were quantified from digital images using image analysis software (Metamorph software). Results are expressed as the

percentage of GFAP and MSA positive area. For each morphometric analysis, a total of 30 high power images from 5 mice per group per time point (2d –8 wks) were analyzed.

Analysis of brain protein extracts

Brain tissue was excised from the implantation site with fine forceps under a dissecting microscope. Tissue was also excised from the controlateral site and served as non-implant control. Brain extracts were prepared from excised tissue via lysis in RIPA buffer. Western blots for MMP-9, IL-10, ZO-1, and ZO-2 were performed according to standard protocols. IL-1β in brain tissue was detected by immunoprecipitation as described previously (Hogquist et al, 1991). Briefly, equal amounts of protein extracts (500 μg) were pre-cleared by protein A-Sepharose incubation for 1 h at 4 °C followed by centrifugation. The cleared lysates were incubated with the same amount of anti-IL-1β mAb (R&D system) for 2 h at 4 °C followed by protein A-Sepharose for an additional 1 h. The immune complexes were washed three times with RIPA buffer, boiled in SDS-PAGE sample buffer for 5 min, and separated by SDS-PAGE (12.5% acrylamide). Proteins were transferred to nitrocellulose membranes and IL-1β was detected with the same antibody (1:1000) with chemoluminescence detection reagent (Western Lightening, Perkin Elmer and MA). For detection of gelatinase activity, 50 μg of brain extracts from WT and MMP-9-null 4 wk implants were analyzed by zymography as described previously (Agah et al., 2004). Quantification of IL-1β by ELISA was performed with a commercially available kit (BD Biosciences) according to the supplier's instructions.

Statistical analysis

All data are expressed as mean ± SEM. Differences between groups were analyzed by student t-test. A p value ≤ 0.05 was considered significant.

Supplementary Material

Refer to Web version on PubMed Central for supplementary material.

Acknowledgments

We thank Eleni Skokos, Jianmin Zeng, and Marie Krady for assistance. We thank Drs. Mark Laubach and Vincent Pieribone for assistance with brain implantations, Dr. Robert Senior for the MMP-9-null mice, and Dr. George Tellides for assistance with IL-1β quantification. This study was supported by National Institute of Health Grant GM 072194-01 (to T.R.K.).

References

Agah A, Kyriakides TR, Letrondo N, Bjorkblom B, Bornstein P. Thrombospondin 2 levels are increased in aged mice: consequences for cutaneous wound healing and angiogenesis. Matrix Biol. 2004; 22:539–547. [PubMed: 14996433]

Agrawal S, Anderson P, Durbeej M, van Rooijen N, Ivars F, Opdenakker G, Sorokin LM. Dystroglycan is selectively cleaved at the parenchymal basement membrane at sites of leukocyte extravasation in experimental autoimmune encephalomyelitis. J Exp Med. 2006; 203:1007–1019. [PubMed: 16585265]

Agrawal SM, Lau L, Yong VW. MMPs in the central nervous system: where the good guys go bad. Sem Cell Dev Biol. 2008; 19:42–51.

Albaiceta GM, Gutierrez-Fernandez A, Parra D, Astudillo A, Garcia-Prieto E, Taboada F, Fueyo A. Lack of matrix metalloproteinase-9 worsens ventilator-induced lung injury. Am J Physiol Lung Cell Mol Physiol. 2008; 294:L535–L543. [PubMed: 18223162]

Anderson JM, Rodriguez A, Chang DT. Foreign body reaction to biomaterials. Sem Immunol. 2008; 20:86–100.

Argaw AT, Zhang YT, Snyder BJ, Zhao ML, Kopp N, Lee SC, Raine CS, Brosnan CF, John GR. IL-1 beta regulates blood-brain barrier permeability via reactivation of the hypoxia-angiogenesis program. J Immunol. 2006; 177:5574–5584. [PubMed: 17015745]

Asahi M, Wang X, Mori T, Sumii T, Jung JC, Moskowitz MA, Fini ME, Lo EH. Effects of matrix metalloproteinase-9 gene knock-out on the proteolysis of blood-brain barrier and white matter components after cerebral ischemia. J Neurosci. 2001; 21:7724–7732. [PubMed: 11567062]

Balasingam V, Dickson K, Brade A, Yong VW. Astrocyte reactivity in neonatal mice: apparent dependence on the presence of reactive microglia/macrophages. Glia. 1996; 18:11–26. [PubMed: 8891688]

Beck DW, Hart MN, Cancilla PA. The role of the macrophage in microvascular regeneration following brain injury. J Neuropathol Exp Neurol. 1983; 42:601–614. [PubMed: 6631454]

Biran R, Martin DC, Tresco PA. Neuronal cell loss accompanies the brain tissue response to chronically implanted silicon microelectrode arrays. Exp Neurol. 2005; 195:115–126. [PubMed: 16045910]

Blight AR. Effects of silica on the outcome from experimental spinal cord injury: implication of macrophages in secondary tissue damage. Neuroscience. 1994; 60:263–273. [PubMed: 8052418]

Bolton SJ, Anthony DC, Perry VH. Loss of the tight junction proteins occludin and zonula occludens-1 from cerebral vascular endothelium during neutrophil-induced blood-brain barrier breakdown in vivo. Neuroscience. 1998; 86:1245–1257. [PubMed: 9697130]

Canete-Soler R, Gui YH, Linask KK, Muschel RJ. Developmental expression of MMP-9 (gelatinase B) mRNA in mouse embryos. Dev Dyn. 1995; 204:30–40. [PubMed: 8563023]

Cheung KC. Implantable microscale neural interfaces. Biomedical Microdevices. 2007; 9:923–938. [PubMed: 17252207]

Copin JC, Gasche Y. Matrix metalloproteinase-9 deficiency has no effect on glial scar formation after transient focal cerebral ischemia in mouse. Brain Res. 2007; 1150:167–173. [PubMed: 17434457]

Coulter KR, Doseff A, Sweeney P, Wang YJ, Marsh CB, Wewers MD, Knoell DL. Opposing effect by cytokines on Fas-mediated apoptosis in A549 lung epithelial cells. Am J Respir Cell Mol Biol. 2002; 26:58–66. [PubMed: 11751204]

Coxon A, Tang T, Mayadas TN. Cytokine-activated endothelial cells delay neutrophil apoptosis in vitro and in vivo: a role for granulocyte/macrophage colony-stimulating factor. J Exp Med. 1999; 190:923–933. [PubMed: 10510082]

Cunningham LA, Wetzel M, Rosenberg GA. Multiple roles for MMPs and TIMPs in cerebral ischemia. Glia. 2005; 50:329–339. [PubMed: 15846802]

Ek CJ, Dziegielewska KM, Stolp H, Saunders NR. Functional effectiveness of the blood brain barrier to small water-soluble molecules in developing and adult opossum (Monodelphis domestica). J Comp Neurol. 2006; 496:13–26. [PubMed: 16528724]

Faulkner JR, Herrmann JE, Woo MJ, Tansey KE, Doan NB, Sofroniew MV. Reactive astrocytes protect tissue and preserve function after spinal cord injury. J Neurosci. 2004; 24:2143–2155. [PubMed: 14999065]

Fournier E, Passirani C, Montero-Menei CN, Benoit JP. Biocompatibility of implantable synthetic polymeric drug carriers: focus on brain biocompatibility. Biomaterials. 2003; 24:3311–3331. [PubMed: 12763459]

Gross B, Bitterman N, Levanon D, Nir I, Harel D. Horseradish peroxidase as a cytochemical marker of blood-brain barrier integrity in oxygen toxicity in the central nervous system. Exp Neurol. 1986; 93:471–480. [PubMed: 3743695]

Gu Z, Kaul M, Yan B, Kridel SJ, Cui J, Strongin A, Smith JW, Liddington RC, Lipton SA. S-nitrosylation of matrix metalloproteinases: signaling pathway to neuronal cell death. Science. 2002; 297:1186–1190. [PubMed: 12183632]

He W, McConnell GC, Bellamkonda RV. Nanoscale laminin coating modulates cortical scarring response around implanted silicon microelectrode arrays. J Neural Eng. 2006; 3:316–326. [PubMed: 17124336]

Hogquist KA, Nett MA, Sheehan KCF, Pendleton KD, Schreiber RD, Chaplin DD. Generation of monoclonal antibodies to murine IL-1 beta and demonstration of IL-1 in vivo. J Immunol. 1991; 146:1534–1540. [PubMed: 1993843]

Ito A, Mukaiyama A, Itoh Y, Nagase H, Thogersen IB, Enghild JJ, Sasaguri Y, Mori Y. Degradation of interleukin 1beta by matrix metalloproteinases. J Biol Chem. 1996; 271:14657–14660. [PubMed: 8663297]

Jacobs TP, Kempski O, McKinley D, Dutka AJ, Hallenbeck JM, Feuerstein G. Blood flow and vascular permeability during motor dysfunction in a rabbit model of spinal cord ischemia. Stroke. 1992; 23:367–373. [PubMed: 1542898]

Jaeger CB, Winn SR, Tresco PA, Aebischer P. Repair of the blood-brain barrier following implantation of polymer capsules. Brain Res. 1991; 551:163–170. [PubMed: 1913150]

Jones JA, McNally AK, Chang DT, Meyerson LAQH, Colton E, Kwon ILK, Matsuda T, Anderson JM. Matrix metalloproteinases and their inhibitors in the foreign body reaction on biomaterials. J Biomed Mat Res Part A. 2008; 84:158–166.

Kajiwara K, Ito H, Fukumoto T. Lymphocyte infiltration into normal rat brain following hyperosmotic blood-brain barrier opening. J Neuroimmunol. 1990; 27:133–140. [PubMed: 2110183]

Kieseier BC, Seifert T, Giovannoni G, Hartung HP. Matrix metalloproteinases in inflammatory demyelination: targets for treatment. Neurology. 1999; 53:20–25. [PubMed: 10408531]

Kim YT, Hitchcock RW, Bridge MJ, Tresco PA. Chronic response of adult rat brain tissue to implants anchored to the skull. Biomaterials. 2004; 25:2229–2237. [PubMed: 14741588]

Kinoh H, Sato H, Tsunezuka Y, Takino T, Kawashima A, Okada Y, Seiki M. MT-MMP, the cell surface activator of proMMP-2 (pro-gelatinase A), is expressed with its substrate in mouse tissue during embryogenesis. J Cell Science. 1996; 109:953–959. [PubMed: 8743942]

Kolaczkowska E, Scislowska-Czarnecka A, Chadzinska M, Plytycz B, van Rooijen N, Opdenakker G, Arnold B. Enhanced early vascular permeability in gelatinase B (MMP-9)-deficient mice: putative contribution of COX-1-derived PGE(2) of macrophage origin. J Leuk Biol. 2006; 80:125–132.

Kyriakides TR, Bornstein P. Matricellular proteins as modulators of wound healing and the foreign body response. Thromb and Haemost. 2003; 90:986–992. [PubMed: 14652628]

Kyriakides TR, Foster MJ, Keeney GE, Tsai A, Giachelli CM, Clark-Lewis I, Rollins BJ, Bornstein P. The CC chemokine ligand, CCL2/MCP1, participates in macrophage fusion and foreign body giant cell formation. Am J Pathol. 2004; 165:2157–2166. [PubMed: 15579457]

Laterra J, Guerin C, Goldstein GW. Astrocytes induce neural microvascular endothelial cells to form capillary-like structures in vitro. J Cell Physiol. 1990; 144:204–215. [PubMed: 2380251]

Lee SR, Lo EH. Induction of caspase-mediated cell death by matrix metalloproteinases in cerebral endothelial cells after hypoxia-reoxygenation. J Cereb Blood Flow Metab. 2004; 24:720–727. [PubMed: 15241180]

Lindberg RL, De Groot CJ, Montagne L, Freitag P, van der Valk P, Kappos L, Leppert D. The expression profile of matrix metalloproteinases (MMPs) and their inhibitors (TIMPs) in lesions and normal appearing white matter of multiple sclerosis. Brain. 2001; 124:1743–1753. [PubMed: 11522577]

Lo EH, Dalkara T, Moskowitz MA. Mechanisms, challenges and opportunities in stroke. Nat Rev Neurosc. 2003; 4:399–415.

Maclauchlan S, Skokos EA, Meznarich N, Zhu DH, Raoof S, Shipley JM, Senior RM, Bornstein P, Kyriakides TR. Macrophage fusion, giant cell formation, and the foreign body response require matrix metalloproteinase 9. J Leukoc Biol. 2009 in press.

McMillan SJ, Kearley J, Campbell JD, Zhu XW, Larbi KY, Shipley JM, Senior RM, Nourshargh S, Lloyd CM. Matrix metalloproteinase-9 deficiency results in enhanced allergen-induced airway inflammation. J Immunol. 2004; 172:2586–2594. [PubMed: 14764732]

Medhora M, Harder D. Functional role of epoxyeicosatrienoic acids and their production in astrocytes: approaches for gene transfer and therapy (review). Int J Mol Med. 1998; 2:661–669. [PubMed: 9850733]

Mitchell J, Weller RO, Evans H. Reestablishment of the blood brain barrier to peroxidase following cold injury to mouse cortex. Acta Neuropathol. 1979; 46:45–49. [PubMed: 452862]

Mun-Bryce S, Rosenberg GA. Gelatinase B modulates selective opening of the blood-brain barrier during inflammation. Am J Physiol. 1998; 274:R1203–1211. [PubMed: 9644031]

Murphy S, Pearce B, Jeremy J, Dandona P. Astrocytes as eicosanoid-producing cells. Glia. 1988; 1:241–245. [PubMed: 2977123]

Nag S, Picard P, Stewart DJ. Expression of nitric oxide synthases and nitrotyrosine during blood-brain barrier breakdown and repair after cold injury. Lab Inv. 2001; 81:41–49.

Nagase H, Woessner JF Jr. Matrix metalloproteinases. J Biol Chem. 1999; 274:21491–21494. [PubMed: 10419448]

Noble LJ, Donovan F, Igarashi T, Goussev S, Werb Z. Matrix metalloproteinases limit functional recovery after spinal cord injury by modulation of early vascular events. J Neurosci. 2002; 22:7526–7535. [PubMed: 12196576]

Noble LJ, Wrathall JR. Distribution and time course of protein extravasation in the rat spinal cord after contusive injury. Brain Res. 1989; 482:57–66. [PubMed: 2706482]

Overall CM, Lopez-Otin C. Strategies for MMP inhibition in cancer: innovations for the post-trial era. Nat Rev Cancer. 2002; 2:657–672. [PubMed: 12209155]

Parks WC, Wilson CL, Lopez-Boado YS. Matrix metalloproteinases as modulators of inflammation and innate immunity. Nat Rev. 2004; 4:617–629.

Polikov VS, Tresco PA, Reichert WM. Response of brain tissue to chronically implanted neural electrodes. J Neurosc Meth. 2005; 148:1–18.

Proost P, Van Damme J, Opdenakker G. Leukocyte gelatinase B cleavage releases encephalitogens from human myelin basic protein. Biochem Biophys Res Commun. 1993; 192:1175–1181. [PubMed: 7685161]

Schenkel AR, Mamdouh Z, Muller WA. Locomotion of monocytes on endothelium is a critical step during extravasation. Nat Immunol. 2004; 5:393–400. [PubMed: 15021878]

Schonbeck U, Mach F, Libby P. Generation of biologically active IL-1 beta by matrix metalloproteinases: a novel caspase-1-independent pathway of IL-1 beta processing. J Immunol. 1998; 161:3340–3346. [PubMed: 9759850]

Shigemori Y, Katayama Y, Mori T, Maeda T, Kawamata T. Matrix metalloproteinase-9 is associated with blood-brain barrier opening and brain edema formation after cortical contusion in rats. Acta Neurochir. 2006; 96:130–133.

Sood RR, Taheri S, Candelario-Jalil E, Estrada EY, Rosenberg GA. Early beneficial effect of matrix metalloproteinase inhibition on blood-brain barrier permeability as measured by magnetic resonance imaging countered by impaired long-term recovery after stroke in rat brain. J Cereb Blood Flow Metab. 2008; 28:431–438. [PubMed: 17700631]

Stolp HB, Dziegielewska KM, Ek CJ, Potter AM, Saunders NR. Long-term changes in blood-brain barrier permeability and white matter following prolonged systemic inflammation in early development in the rat. Eur J Neurosc. 2005; 22:2805–2816.

Suarez I, Bodega G, Rubio M, Garcia-Segura LM, Fernandez B. Astroglial induction of in vivo angiogenesis. Journal of neural transplantation & plasticity. 1994; 5:1–10. [PubMed: 7529564]

Szarowski DH, Andersen MD, Retterer S, Spence AJ, Isaacson M, Craighead HG, Turner JN, Shain W. Brain responses to micro-machined silicon devices. Brain Res. 2003; 983:23–35. [PubMed: 12914963]

Tang J, Liu J, Zhou C, Alexander JS, Nanda A, Granger DN, Zhang JH. Mmp-9 deficiency enhances collagenase-induced intracerebral hemorrhage and brain injury in mutant mice. J Cereb Blood Flow Metab. 2004; 24:1133–1145. [PubMed: 15529013]

Tator CH, Fehlings MG. Review of the secondary injury theory of acute spinal cord trauma with emphasis on vascular mechanisms. J Neurosurg. 1991; 75:15–26. [PubMed: 2045903]

van Vliet EA, Araujo SD, Redeker S, van Schaik R, Aronica E, Gorter JA. Blood-brain barrier leakage may lead to progression of temporal lobe epilepsy. Brain. 2007; 130:521–534. [PubMed: 17124188]

Visse R, Nagase H. Matrix metalloproteinases and tissue inhibitors of metalloproteinases: structure, function, and biochemistry. Circ Res. 2003; 92:827–839. [PubMed: 12730128]

Vu TH, Shipley JM, Bergers G, Berger JE, Helms JA, Hanahan D, Shapiro SD, Senior RM, Werb Z. MMP-9/gelatinase B is a key regulator of growth plate angiogenesis and apoptosis of hypertrophic chondrocytes. Cell. 1998; 93:411–422. [PubMed: 9590175]

Wang M, Qin X, Mudgett JS, Ferguson TA, Senior RM, Welgus HG. Matrix metalloproteinase deficiencies affect contact hypersensitivity: stromelysin-1 deficiency prevents the response and

gelatinase B deficiency prolongs the response. Proc Natl Acad Sci U S A. 1999; 96:6885–6889. [PubMed: 10359808]

Wang P, Dai J, Bai F, Kong KF, Wong SJ, Montgomery RR, Madri JA, Fikrig E. Matrix metalloproteinase 9 facilitates West Nile virus entry into the brain. J Virol. 2008; 82:8978–8985. [PubMed: 18632868]

Wang X, Jung J, Asahi M, Chwang W, Russo L, Moskowitz MA, Dixon CE, Fini ME, Lo EH. Effects of matrix metalloproteinase-9 gene knock-out on morphological and motor outcomes after traumatic brain injury. J Neurosci. 2000; 20:7037–7042. [PubMed: 10995849]

Wijsman JA, Shivers RR. Heat stress affects blood-brain barrier permeability to horseradish peroxidase in mice. Acta Neuropathol. 1993; 86:49–54. [PubMed: 8372642]

Williams KC, Hickey WF. Traffic of hematogenous cells through the central nervous system. Curr Top Microbiol Immunol. 1995; 202:221–245. [PubMed: 7587365]

Yang Y, Estrada EY, Thompson JF, Liu W, Rosenberg GA. Matrix metalloproteinase-mediated disruption of tight junction proteins in cerebral vessels is reversed by synthetic matrix metalloproteinase inhibitor in focal ischemia in rat. J Cereb Blood Flow Metab. 2007; 27:697–709. [PubMed: 16850029]

Yong VW. Metalloproteinases: mediators of pathology and regeneration in the CNS. Nat Rev Neurosci. 2005; 6:931–944. [PubMed: 16288297]

Yoshizumi H, Fujibayashi Y, Kikuchi H. A new approach to the integrity of dual blood-brain barrier functions of global ischemic rats. Barrier and carrier functions. Stroke. 1993; 24:279–284. discussion 284-275. [PubMed: 8421829]

Zhao BQ, Wang S, Kim HY, Storrie H, Rosen BR, Mooney DJ, Wang X, Lo EH. Role of matrix metalloproteinases in delayed cortical responses after stroke. Nat Med. 2006; 12:441–445. [PubMed: 16565723]

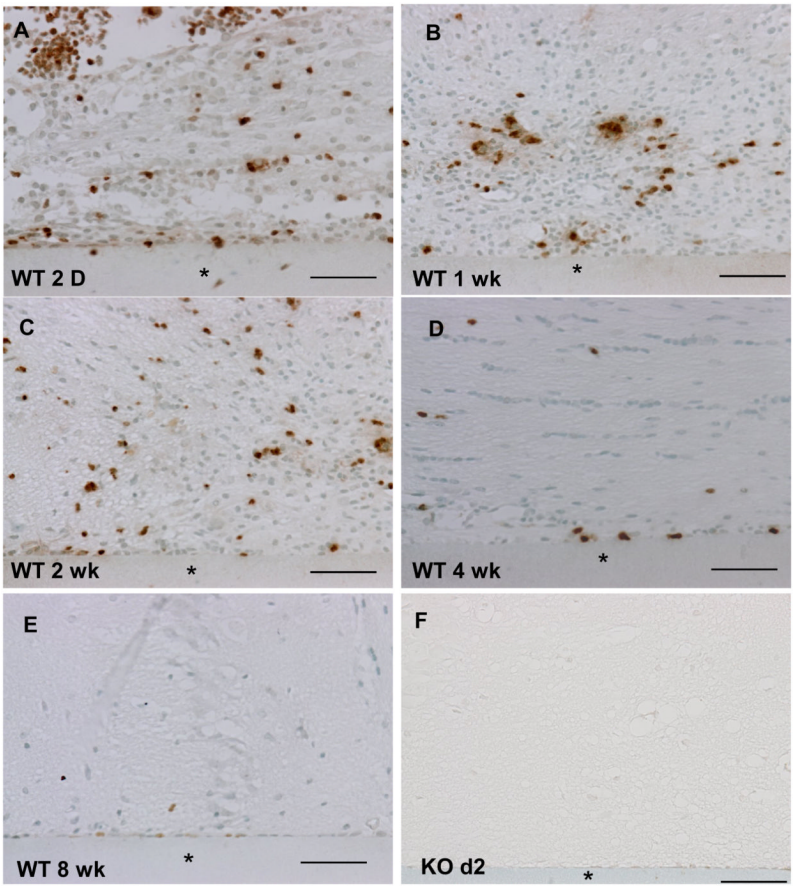

Figure 1. MMP-9 deposition after implantation in the brain cortex

Representative sections of implants (*) from WT (A-E) and from MMP-9-null mice (F) were stained with an anti-MMP-9 Ab and visualized with the peroxidase reaction (brown color). MMP-9 deposition was observed at 2d post implantation (A) and remained high at 1 (B) and 2 wk (C). The deposition was detectable but decreased at 4 (D) and 8 wk (E). Scale bar = 50μm.

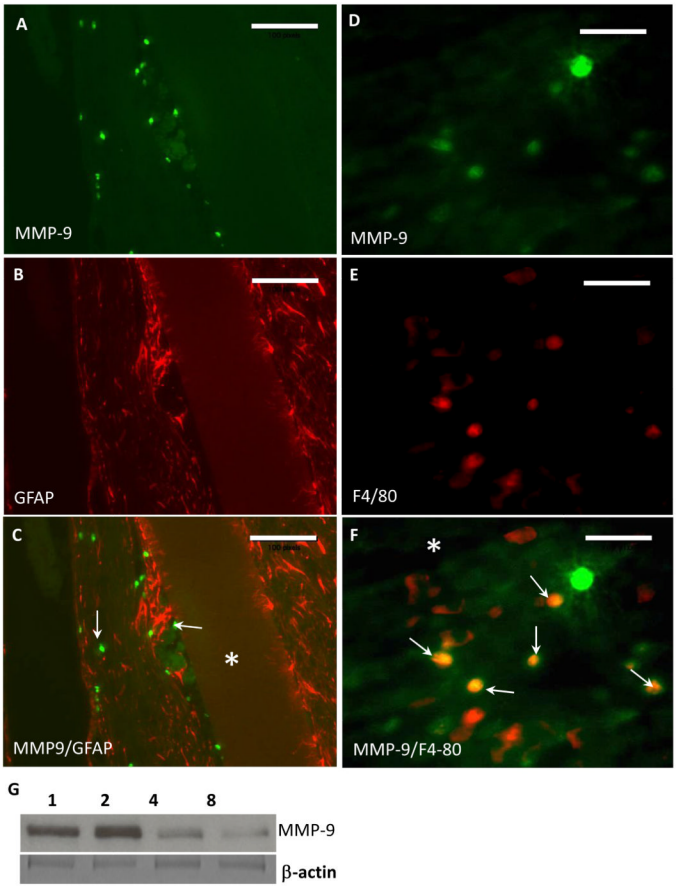

Figure 2. MMP-9 co-localization with macrophages during the foreign body response

Representative images from 2 wk implants in WT mice stained with anti-MMP-9 (A, D), GFAP (B), and F4/80 (D) are shown. (C) Merge of images A and B. Arrows denote MMP-9-positive cells. (F) Merge of images B and D. Arrows denote overlap between MMP-9 and F4/80 imunoreactivity. Implant location is denoted by an asterisk. (G) Western blot of brain extracts showing the presence of MMP-9 at 1, 2, 4, and 8 wk. Bottom image shows β-actin immunostain as loading control. Scale Bar = 200 μm (A-C), 50 μm (D-F).

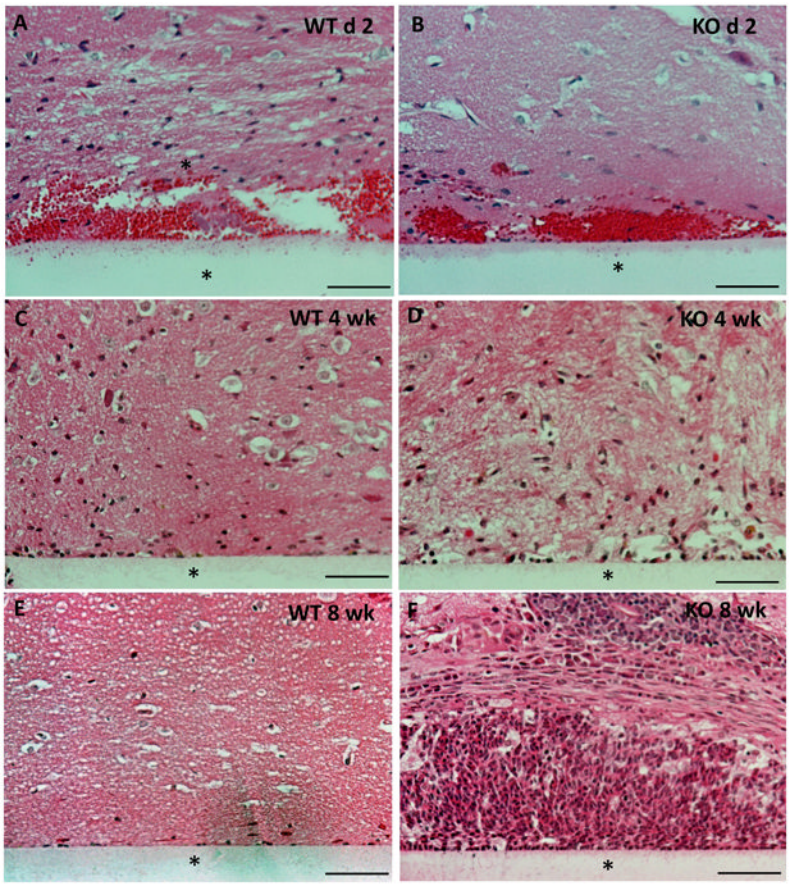

Figure 3. Increased cellular accumulation following implantation in MMP-9-null mice

Representative images of implants (*) implanted in the brain cortex for a period of 2 d -8 wk and stained with H&E are shown. Unlike WT mice, where the cellular reaction decreased by 4 wk (C), the MMP-9 -null mice displayed a continuous increase in cell accumulation up to 8 wk (F). Scale bar = 50μm.

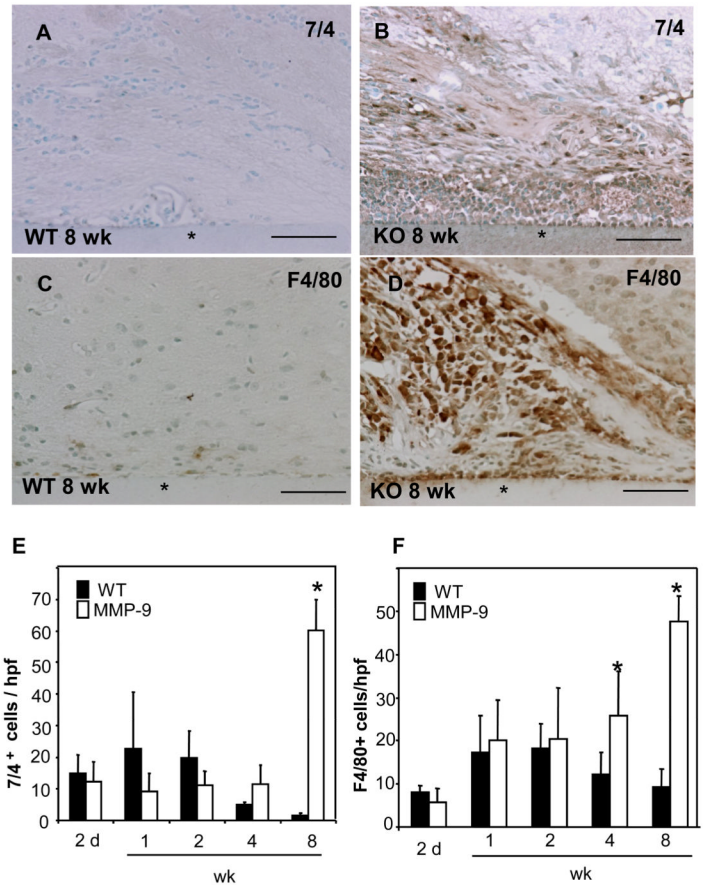

Figure 4. Prolonged neuroinflammation during the FBR in MMP-9-null mice

Representative sections of 8 wk implants (*) from WT (A,C) and MMP-9-null (B,D) mice stained with anti-7/4 Ab (A and B), with F4/80 Ab (C and D) and visualized with the peroxidase reaction are shown (brown color). The numbers of neutrophils (E) and macrophage/microglia (F) per high power field (hpf) were determined from digital images. *p value < 0.05. Scale bar = 50μm.

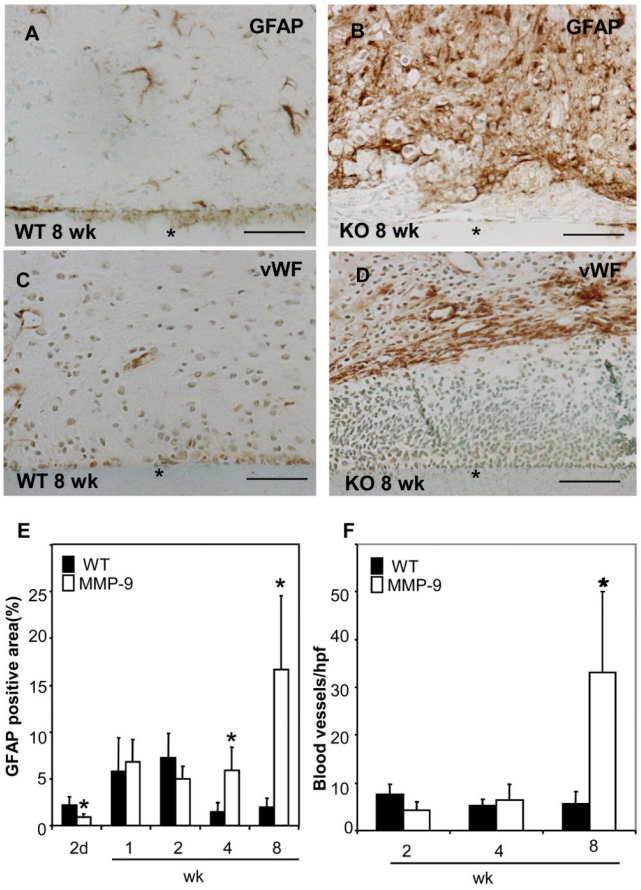

Figure 5. Enhanced astrocyte reaction and angiogenesis in MMP-9-null mice

Representative sections of 8 wk implants (*) from WT (A, C) and MMP-9 -null (B, D) mice were stained with GFAP (A, B) and vWF (C, D) and visualized with the peroxidase reaction (brown color). (E) GFAP deposition was evaluated by morphometric analysis of stained sections and found to be increased at 4 and 8 wk in MMP-9-null mice. **(F)** The number of blood vessels at the implantation site were enumerated and found to be increased in MMP-9-null mice at 8 wk. *p value <0.05. Scale bar = 50μm.

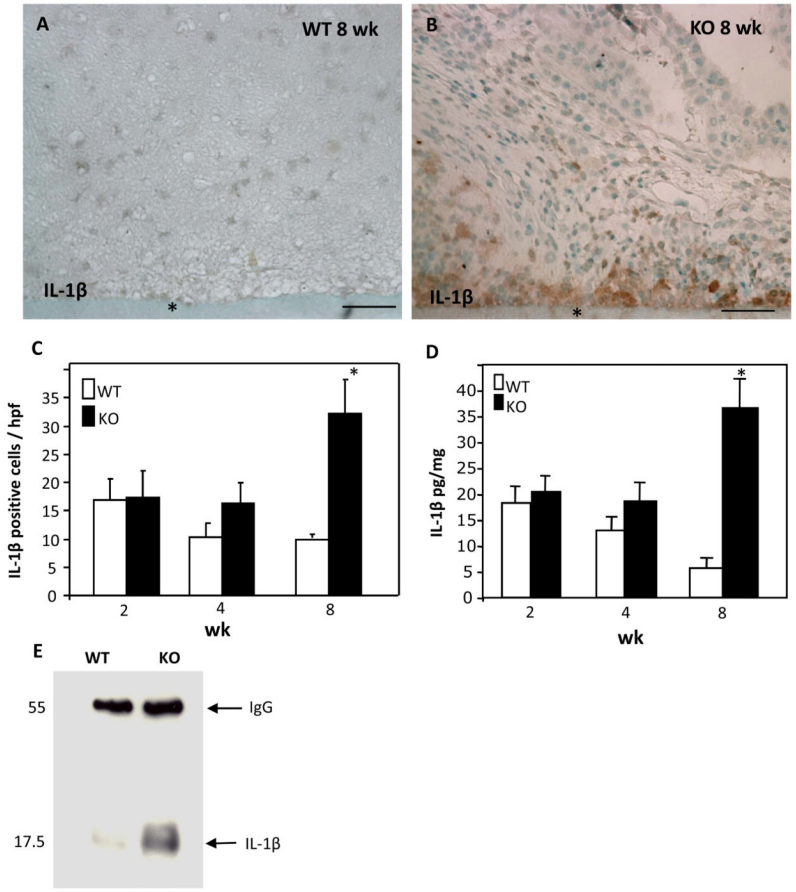

Figure 6. Increased IL-1p levels in MMP-9-null mice

Representative images of sections from WT (A) and MMP-9-null (B) mice at 8 wk following implantation stained with anti- IL-1β Ab and visualized with the peroxidase reaction (brown color). (C) The number of IL-1β expressing cells was enumerated and found to be higher in MMP-9-null mice at 8 wk post-implantation. (D) ELISA analysis of brain extracts revealed increased IL-1β in MMP-9-null mice at 8 wk. (E) Immunoprecipitation of brain extracts from mice harboring implants for 8 wk showed increased levels of IL-1β in MMP-9-null mice. *p value <0.05 (C, D). Scale bar = 50μm (A, B).

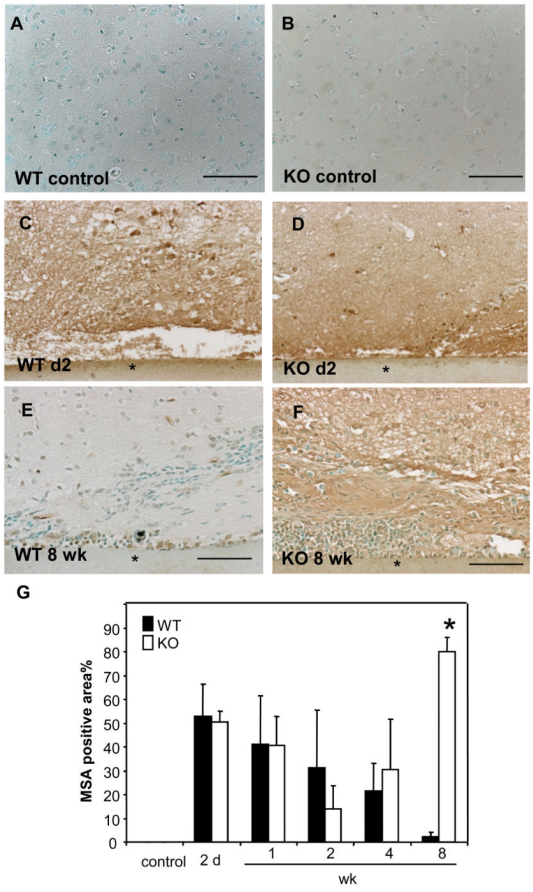

Figure 7. Prolonged BBB leakage in MMP-9-null mice

Representative images of implants from WT (A, C, E), MMP-9 -null (B, D, F) mice stained with anti-MSA Ab and visualized with the peroxidase reaction (brown color) are shown. (G) Extravasated mouse serum albumin (MSA) was evaluated by morphometric analysis of stained sections using Metamorph and suggested complete repair in WT mice. In contrast, repair of the BBB in MMP-9-null was compromised. * p value <0.05. Scale bar = 50μm (A-F).

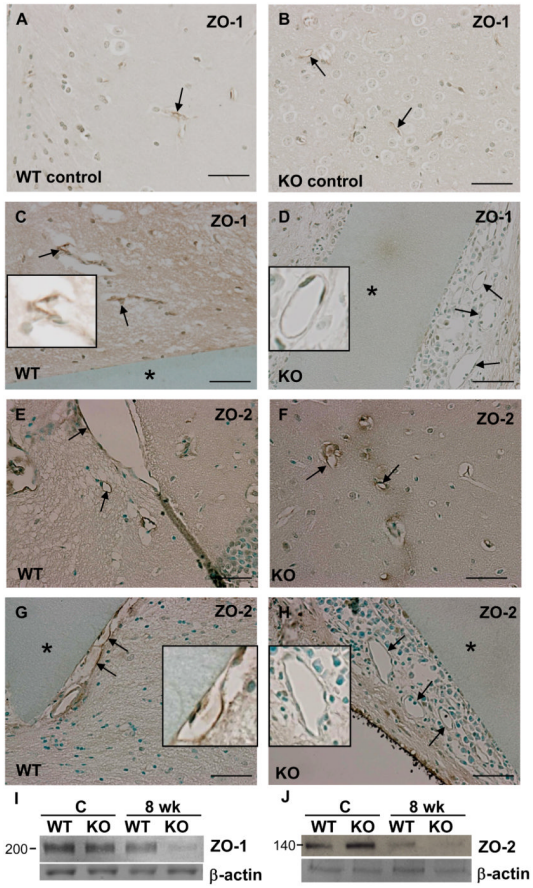

Figure 8. Loss of ZO-1 and ZO-2 in MMP-9-null blood vessels

Immunohistohemical detection of ZO-1 (A-D) and ZO-2 (E-H) in sections from mice with 8 wk implants (*) (C, D, G, H) or without (A, B, E, F). Images from WT (A, C, E, G) and MMP-9-null mice (B, D, F, H) are shown and arrows denote blood vessels. Compared with WT mice, ZO-1 and ZO-2 were absent from the blood vessels adjacent to the implants in MMP-9-null mice (D, H). Insets show close-ups of individual vessels. (I, J) Western blot analysis of ZO-1 and ZO-2 in brain extracts from control and 8 wk implants in WT and MMP-9-null (KO) mice. Results are representative of two independent experiments. Scale bar = 50μm (A-H).